The International Journal Of Engineering And Science (IJES)
|| Volume || 5 || Issue || 10 || Pages || PP 41-51 || 2016 ||
ISSN (e): 2319 – 1813 ISSN (p): 2319 – 1805

Characterization of Aluminum Doped Nanostructured ZnO/p-Si Heterojunctions

A. Kaphle[1] and P. Hari[1]
[1.] *Department of Physics and Engineering Physics, The University of Tulsa, Tulsa, OK USA, 74104*

ABSTRACT
In this study we investigated electrical and optical properties of heterojunctions made of aluminum doped Zinc oxide (ZnO) nanorods and 4% Boron doped p-type silicon (p-Si). ZnOnanorods were grown by a chemical bath deposition (CBD) techniqueon a seed layer of ZnOsputtered on p-Si. Aluminum doping was achieved by incorporating 0-20% of aluminum nitrate in the chemical bath precursor solution. Room temperature photoluminescence showed a systematic decrease in the defect peak at 560 nm with increasing doping. Band gap was measured using UV-VIS spectroscopy shows that the band gap increased from 3.31 eV to 3.58 eV as the doping is varied from 0-20%. This increase in band gap could be due to the Burstein-Moss effect previously observed in heavily doped semiconductors. In addition, we also performed current-voltage (I-V), capacitance-voltage(C-V) measurements on Aluminum doped ZnO/p-Si nanorods samples under both dark and illumination conditions. I-V characteristics showed a good rectifying behavior under dark and illumination conditions. The saturation current, diode ideality factor, carrier concentrations, built in potential, and barrier height were calculated from I-V and C-V measurements for each sample. We will discuss the implications of the variations in band gap, I-V, and C-V measurements with variation in aluminum doping.

Keywords:Aluminum, doping**,**Band gap, Barrier height, Ideality factor, ZnO nanorods

Date of Submission: 17 May 2016 Date of Accepted: 18 October 2016

I. INTRODUCTION

In recent years, zinc oxide (ZnO) nanostructures have attracted a lot of interest due to their novel semiconducting, piezoelectric, and optical properties together with the potential applications at high temperatures and harsh environments. ZnO offers a wide variety of morphologies, for instance, in the form of nano needles (NNs), nanowires, and nanorods [1]. Nanostructured ZnO is a promising candidate for optoelectronic application because of its wide band gap of 3.37eV.In addition, nanostructured ZnO has a large surface-to-volume ratio compared to bulk ZnO. These properties result in enhanced light absorption in the UV region which in turn enhances the photo response of nanostructured ZnO devices. Due to the presence of oxygen vacancies and zinc interstitials, ZnO is intrinsically an-type semiconductor [2]. Electrical conduction propertiesof ZnOcan be controlled by doping with of transition metals resulting in doped materials that are highly conductive. Aluminum or Indium doped ZnO has been previously used as a transparent conducting oxide (TCO) in electrodes for solar cells and flat panel display [3].

II. LITERATURE SURVEY

There are many challenges in creating a doped ZnO. Because of low dissolvability of dopants, most ZnO based optoelectronic devices depend on the choice of heterojunctions between ann-type ZnO and a p-type semiconducting material. The most widely used choice for optoelectronic application is the p-type silicon. P-Si/n-ZnO heterojunction have been previously utilized as UV visible photo detectors [4,5], light emitting diodes (LEDs) [6] and solar cells [3]. There are only few studies reported on electrical and optoelectronic properties of ZnO nanostructure based heterojunctions [1]. Al-Henini et al. [7] considered the electrical properties of the p-Si/n-ZnO nanowires heterojunction. Guo et al. [8] have created ZnO nanowires/n-Si heterojunction by utilizing magnetron cosputtering strategy and have shown a solid responsivity of the junction for both visible and UV light. Recently, Li et al. [9] have fabricated n-ZnO/p-Si heterojunction by utilizing a plasma-assisted sub-atomic bar epitaxy method and have additionally exhibited a solid responsivity of the n-ZnO/p-Si heterojunction to both the visible and UV light. He et al.[10] concentrated on the electrical and photoelectrical execution of nano photodiodes based on ZnO nanowires/p-Si heterojunction.

III. RESEARCH ELABORATIONS

Several techniques were used to grow nanostructured n-type ZnO. These include sol–gel process [11], chemical vapor deposition [12], sputtering [13], spray pyrolysis [14], and chemical bath deposition [15]. There are few reports on the properties of ZnO nanorods/p-Si heterojunction prepared by chemical bath deposition. The present study deals with the electrical, optical and structural propertiesof n-ZnO/p-Si heterojunction, where ZnOnanorods were grown by a low cost and simple technique such as chemical bath deposition. The initial segment of this work describes the structural and optical properties investigations of aluminum doped ZnO nanorods. In particular, the impact of aluminum doping on the photoluminescence (PL) properties of ZnO. In the later part, electrical characterizations by current–voltage (I-V) and capacitance–voltage (C-V) measurements on doped ZnO at various temperatures are described.

IV. EXPERIMENTAL

Doped and undopedZnOnanorods were grown on Boron doped (4%) p type Si wafers by chemical bath deposition method. The chemicals zinc nitrate hexahydrate [Zn(CH3COO) 2·2H2O, >99.5%], aluminum nitrate nonahydrate [Co(CH3COO)2·2H2O, >98%], hexamethyltetramine [$C_6H_{12}N_4$, >98%] were purchased from Sigma Aldrich. Before deposition, the silicon (Si) substrates were first cleaned in a sequence with dilute HCL, acetone, isopropanol, and de-ionized water.

2.1 Seed layer deposition:

A 200 nm thick layer of ZnO was deposited as a seed layer on silicon substrate using sputtering technique with zinc target and annealed in air ambient for 2 hours to get ZnO layer. The buffer seed layer facilitates subsequent growth of ZnO nanorods and controls the growth orientation of the nanorods.

2.2 Preparation of ZnO nanorods:

The ZnO NRs were prepared using chemical bath deposition technique with an aqueous solution of zinc nitrate hexahydrate [Zn $(NO_3)_2 \cdot 6H_2O$, 0.05M] and hexamethyltetramine (HMT) [C6H12N4, 0.05 M]. In addition, to prepare Al doped ZnO, aluminum nitrate nonahydrate [Zn(NO3)3·9H2O] was used as doping agent with different Al/Zn molar ratios of Al^{+3}/Zn^{+2} = 5%, 10%, 15%, 20%.The prepared seed layers' substrate was kept in the solution for 6 h at 90 °C. After the chemical bath treatment, the samples were washed several times using deionized water and dried. Finally, the films were annealed at 300 °C for 2 h.

2.3 Characterization:

Structural characterization of prepared ZnO nanorods was done by scanning electron microscopy (SEM) analysis. The absorption and transmission spectra of the samples were measured by a UV–Vis spectrometer. Room temperature PL spectra were measured using Jasco FP6500 Spectrofluorometer. The thickness of seed layer was measured using GaertnerEllipsometer. The current–voltage (I-V) characteristics of the cells were measured from Keithley 2400 source meter. For illumination, AM 1.5 Global spectrum was used. Capacitance-Voltage (C-V) measurements were taken using 590CV analyzer.

V. RESULT AND DISCUSSION

3.1SEM Analysis:

Scanning Electron Microscope was used to study morphological variations in aluminum doped ZnOnanorods (ZnO NR). Fig. 1(a) and 1(b) shows SEM images of undoped and 15% aluminum doped ZnO nanorods deposited on p-Si. SEM images show highly dense distribution of perpendicularly aligned hexagonal shaped ZnO NRs. The average diameter of the NRs with aluminum doping is plotted in Fig. 2. Fig. 2 shows that the average diameter of the NRs decreased from 96.25 nm to 70.75 nm with increasing aluminum concentration 0-20%. Ionic radii difference betweenAl^{3+} (0.054 nm) and Zn^{2+} (0.074 nm) could be an important factor in influencing the diameter of nanorods [16]. In addition, the existence of Aluminum in ZnO lattice may influence the attractive force between atoms and thus reduce the diameter of ZnO with higher doping.

3.2 Absorption, Transmission, and Band gap:

Fig. 3(a) and 3(b) show the UV-visible absorption and transmission spectra of ZnO NRs with aluminum doping. We observe that the transmission of the film in the visible range was improved by aluminum doping with an average transmission enhancement to 85-90 % for 20% doped compared to 60-65% for the undopedZnO. Optical transmission could be further enhanced by aluminum doping. This improvement in optical transmission may be due to the reduction of intrinsic defect such as oxygen vacancies and zinc interstitials in doped samples

[17]. In addition, enhancement in optical transmission might be due to high degree of vertical alignment, low surface roughness, and uniformity of the film as doping level is increased [18].

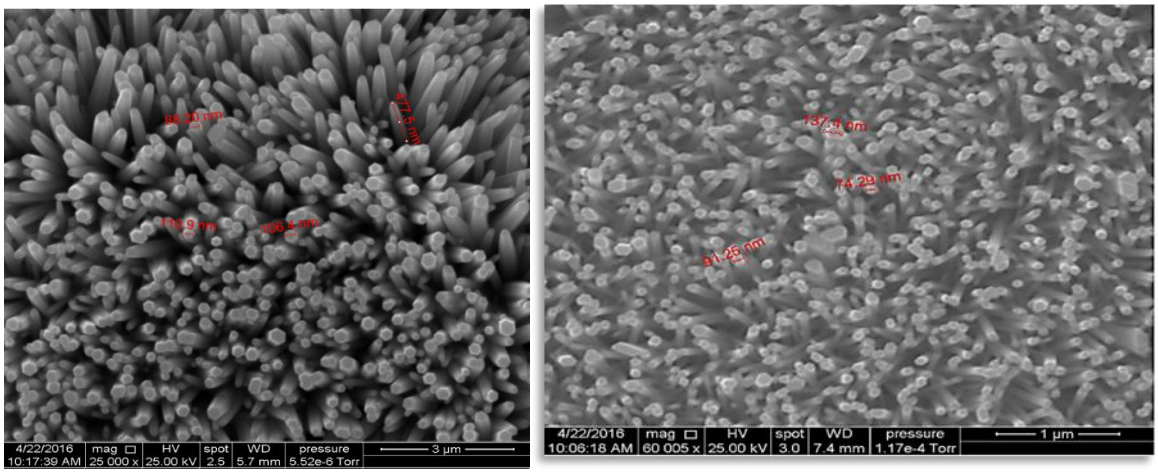

(a) **(b)**

Fig. 1 ZnO NRs grown on p-Si (a) undoped (b) 15% Al doped

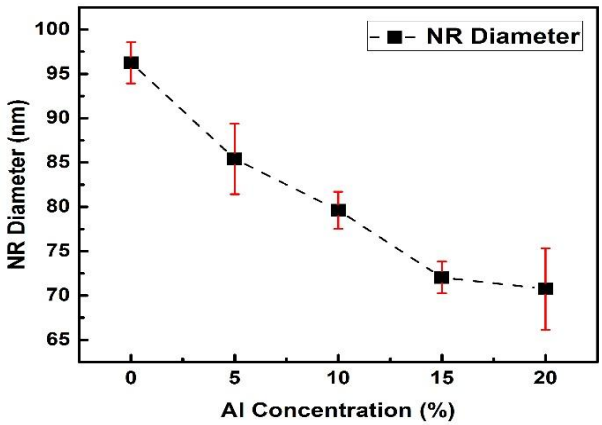

Fig. 2 Variation of ZnO NRs diameter with Aluminum doping

The estimated band gap for all the samples were calculated using the following equation

$$(\alpha h\nu) = A\,(h\nu - Eg)^n \qquad (1)$$

Where h is the Plank's constant, ν is the photon frequency; A is a constant, Eg is the band-gap and n is the index which depends on the type of transition. For direct band-gap semiconductor n value is 1/2, and 2 for an indirect band-gap semiconductor. Thus, the optical band gap can be estimated from $(\alpha h\nu)^2$ vs. hν plot as shown in the Fig. 4.

The standard value of the optical band-gap value for undoped single crystal ZnO is 3.31 eV. The band-gap value was found to increases to 3.58 eV with increasing aluminum concentration (20%), as shown in Fig 5. The band gap broadening can be explained by Burstein Moss (BM) effect. According to the Burstein-Moss effect [19, 20], the broadening of the optical band gap is given as follow

$$\Delta E_g = \left(\frac{h^2}{2m_{vc}^*}\right)(3\pi^2 n)^{\frac{2}{3}} \qquad (2)$$

Where ΔEg is the energy shift of the doped sample compared to undoped sample, m_{vc}^* is the reduced effective mass, h is the Plank constant, and n is the carrier concentration. Based on this condition, the optical band gap would increase with increasing carrier concentration [21].

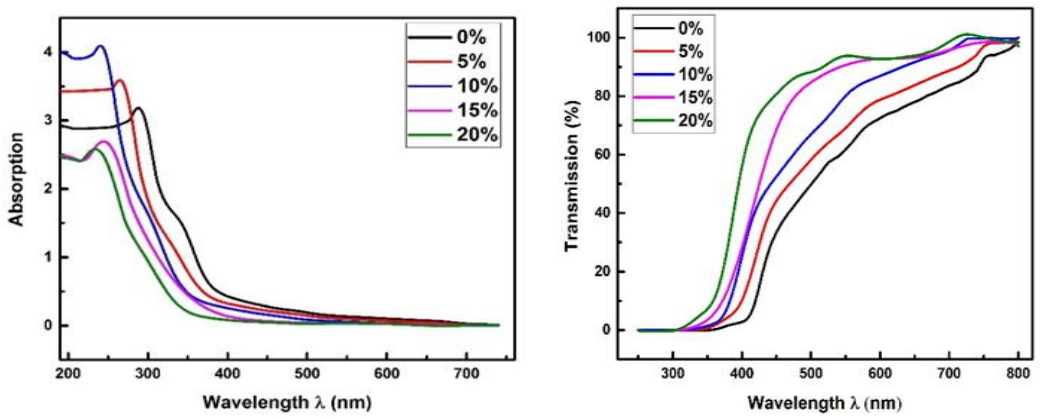

(a) **(b)**

Fig. 3(a) Absorption and **(b)** Transmission spectra of ZnO NRs for different doped samples

3.3 Photoluminescence:

Fig. 6 (a)) shows that the PL spectrum in doped and undopedZnOnanorods samples exhibit three characteristic peaks one is in the UV range and the other two in the visible range. The peak in the UV region corresponds to the near band edge (NBE), attributed to the radiative recombination of free excitons, and the peaks in the visible region are associated with structural defects such as Zn interstitials and oxygen vacancies [22]. PL peak at 470 nm and the green band emission at 560 nm were significantly reduced by aluminum doping. It is very likely that addition of Aluminum into highly defective ZnOnanorods leads to decrease in the number of defects such as oxygen vacancies. A similar result was reported by Lin et al. [23].

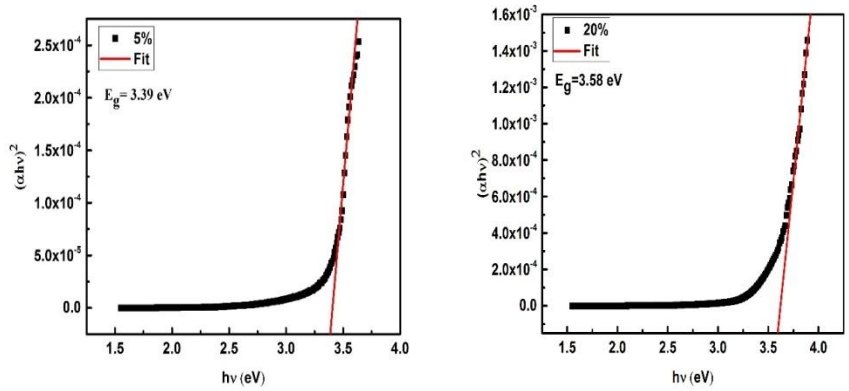

(a) (b)

Fig. 4 Tauc plot to find band gap **(a)** 5% **(b)** 20% aluminum doped samples

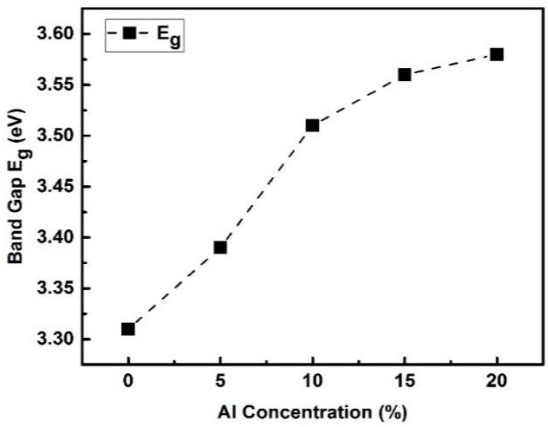

Fig. 5 Band gap variation with aluminum doping

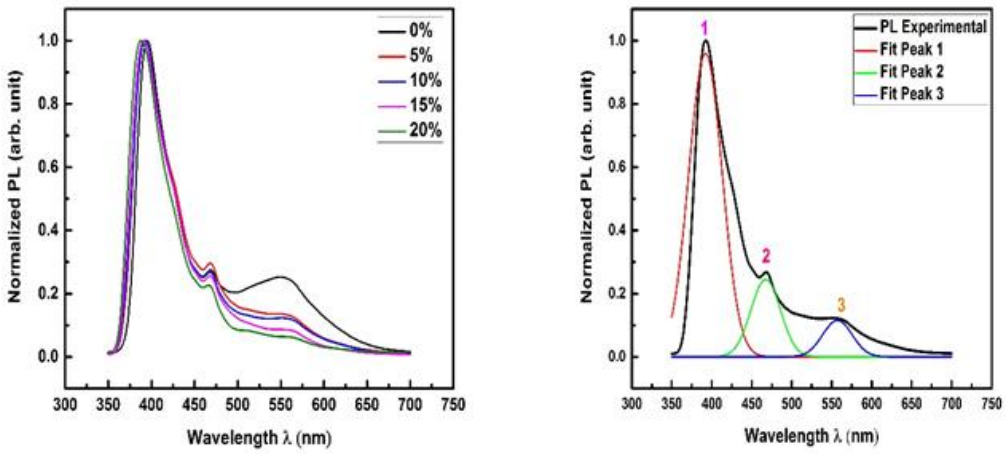

(a) **(b)**

Fig. 6 (a) Photoluminescence spectra of 0-20% aluminum doped ZnO NRs **(b)** Gaussian fit of 10% aluminum doped samples

It has been proposed that at high dopant concentrations, impurity band merge with valence band edge and it becomes band tail states at higher doping concentration. Because of this effect the optical transition between conduction and valence band is increased with doping concentrations, and we observed a corresponding increase in full width at half maximum (FWHM) of the PL (Fig. 7a). It can be seen from fig. 7 (b) that the peak intensity of UV emission varies with Al concentrations. The ZnO nanorods doped with 20 % Al shows strong UV emission and high intensity ratio of UV to visible emission (I_{UV}/I_{VIS}) as compared to other concentrations of Aluminum. This may be due to addition of Al into ZnO nanorods leads to decrease of the number of defects [24]. These analysis shows that aluminum doping improved the optical properties of ZnOnanorods.

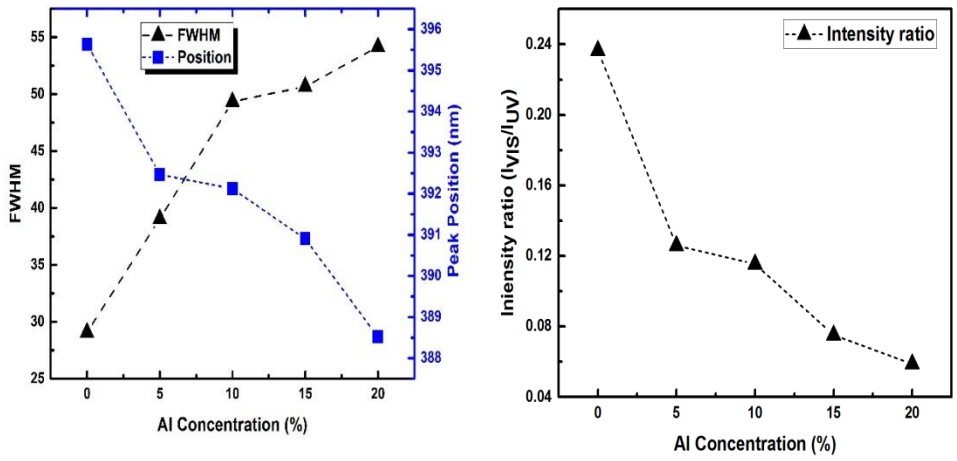

(a) **(b)**

Fig. 7(a) Variation of FWHM and Peak position with aluminum doping **(b)** Intensity ratio as a function of doping concentration.

3.4 Current-Voltage (I-V) measurement:

Fig. 8(a) shows the current-voltage (I-V) characteristics of the p-Si/ZnO heterojunction under both dark and illumination conditions. I-V characteristic shows that the p-n junction shows strong rectification properties with doping. The photocurrent of doped ZnO after 5% decreases due to excessive Aluminum produces the defects which influenced electron mobility and thus resulted in a decreases in photocurrent with higher aluminum concentration. From this result we conclude that the increase in Aluminum content might create more trap levels, compared to the undopedZnO. The rectification ratio (RR) estimated from the I–V characteristic, is found to be 16.11 at ±3 V for undoped samples shown in fig. 8(b). The turn on voltage is around 1 V at room temperature. This value is comparable to the value reported by Mridha and Basak [5] using sol–gel deposition

method for the fabrication of an-ZnO/p-Si heterojunction [25]. There is an increase in RR with doping up to 5% doping level and then RR drops to a lower value at 20%.

The semi-log plot of the dark I–V–T curve (300 to 400K) in Fig. 5 shows two different regions in forward biased condition. At a very low voltage (0<V<0.2), a nearly linear dependence of the current on the voltage was observed. A linear fit ofthe curve to the standard diode equation was used to extract the ideality factor(n), saturation current, and barrier height . The standard diode equation is given by:

$$I = I_0\left(exp\left(\frac{qV}{nkT}\right) - 1\right) \qquad (3)$$

where q is the charge, V is the voltage, k the Boltzmann's constant and T is the temperature in Kelvin. The ideality factor equation is given by;

$$n = \frac{q}{kT \times Slope\ of\ I-V\ Curve} \qquad (4)$$

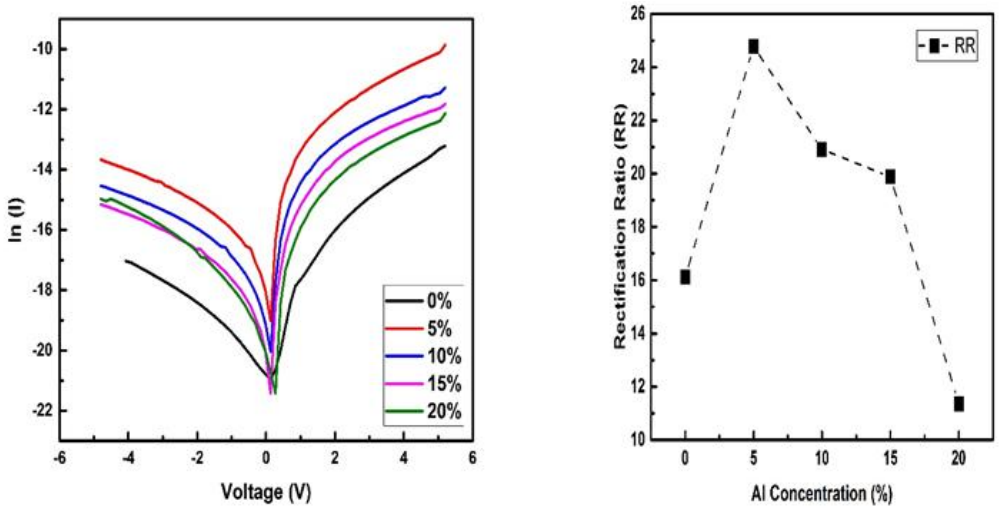

(a) **(b)**

Fig. 8 (a) dark IV characteristics**(b)** Rectification ratio at ±3V.

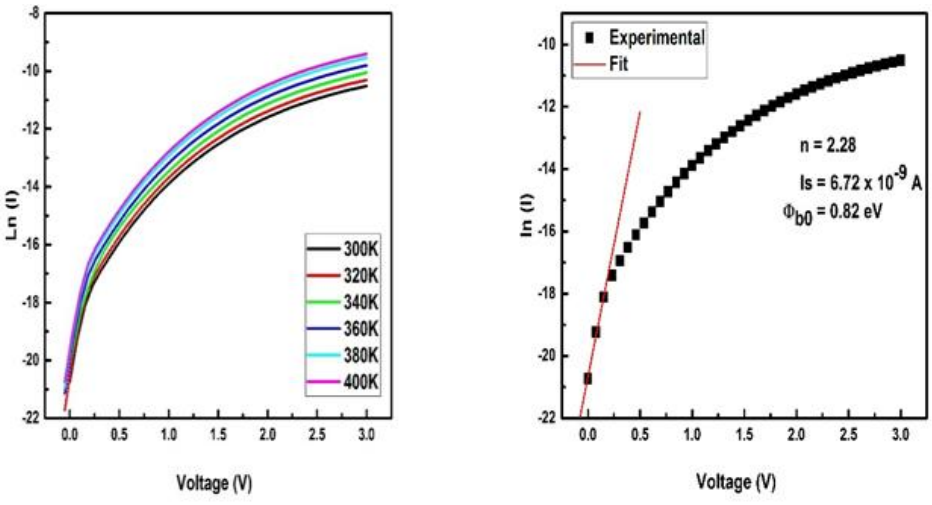

(a) (b)

Fig. 9 (a) Semi log I-V-T plot **(b)** fit to calculate the diode parameter for undoped ZnO

The temperature-dependent saturation current is related to the effective barrier height φ_{b0} by the relation:

$$I = I_0(T)AA^*T^2 exp\left(\frac{q\emptyset_{b0}}{kT}\right) \qquad (5)$$

where, *A* and *A*∗are the contact area and Richardson constant respectively and ϕ_{b0} is the effective barrier height.

Fig. 10 shows ideality factor and barrier height as a function of temperature for undoped ZnO. Both ideality factor and barrier height decreases with increasing temperature. Increase in carrier concentration with increasing temp decreases the parasitic resistance which leads to decrease in ideality factor. It has been suggested that a distribution of inhomogeneity can be modeled by assuming a Gaussian distribution of barrier height in doped ZnO samples [27]. This distribution in barrier height could result in a monotonic decrease in ideality factor with increasing temperature. Similar result was obtained for all other doped (5-20%) samples.

After taking the natural log of (5) we obtain

$$ln(\frac{J_S}{T^2}) = ln(A^*) - \frac{q\phi_{b0}}{kT} \qquad (6)$$

$ln(\frac{J_S}{T^2})$vsq/kTplot gives barrier height and Richardson constant from slope and intercept. The value obtained for Richardson constant based on this analysis results in a very low (1.67 x 10^{-5} A cm^{-2} K^{-1})compared to the standard value of the Richardson constant of 32 A cm^{-2} K^{-2} for undopedZnO [26].

This deviation of Richardson constant from the standard value may be due to barrier inhomogeneity at junction interface [2 7]. The barrier inhomogeneity fluctuation can be modeled by a Gaussian distribution of barrier height with standard deviation σ_0 and average barrier height$\overline{\phi_{b0}}$ [27] can be expressed as

$$\phi_{b0} = \overline{\phi_{b0}} - \frac{q\sigma_0^2}{2kT} \qquad (7)$$

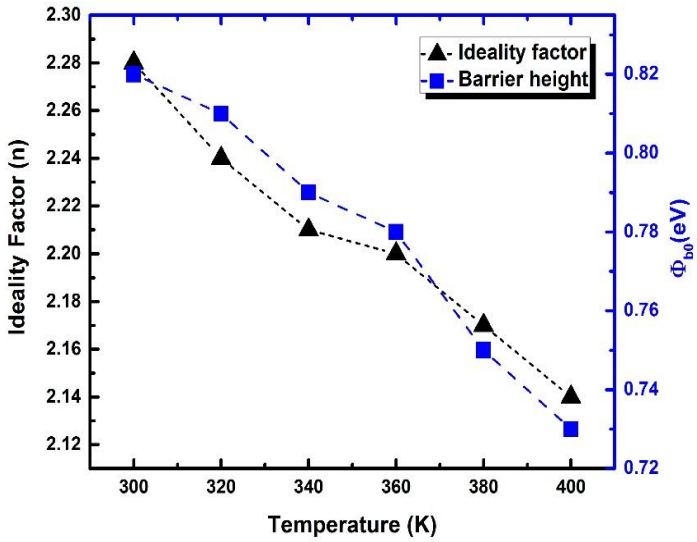

Fig. 10 Ideality factor and barrier height variation with temperature (300K – 400K) for undoped ZnO/p-Si Heterojunction

The modified Richardson equation, taking into account the in homogeneities of the barrier height is given by,

$$\ln\left(\frac{Js}{T^2}\right) - \frac{q^2\sigma_0^2}{2k^2T^2} = ln\,(A^*) - \frac{q\overline{\phi_{b0}}}{kT} \qquad (8)$$

By considering barrier height inhomogeneity and applied modified Richardson equation we obtained a Richardson constant values of 42.84 A cm^{-2} K^{-2}, which is close to theoretical value. Fig.11 (a) shows the Richardson plotand Fig. 11 (b) the modified Richardson plot. Similar procedure was employed for other doped samples.

Ideality factor we obtain from this analysis is greater than one, which is indicative of structural deficiencies in a material. There are number of factors that can account for the increase in the ideality factor. The presence of an interfacial layer, image force lowering of built in potential, recombination of electrons and holes in depletion region and tunneling effect are some of the factors that result in the deviation of the ideality factor from unity [28].

We further observe that the ideality factor decreases from 2.28 to 2.12 as the doping is varied to 5% in Al doped ZnOdoped sample. As the doping is increased beyond 5%, resulting in further increase inideality factor, As the doping is increased, Table 1 shows that the ideality factor is not stabilized. This may be an indication of the changing recombination on rate or the degradation of the junction with higher Al doping [29]. Also, the inhomogeneous thickness of ZnO NRs and non-uniformity of interfacial charges leads to increase in ideality factor and decrease in barrier height beyond 5% aluminum doping.

One interesting result from this analysis is that the barrier height is increased by aluminum doping only up to 5%. After 5% doping, barrier height decreases in all aluminum doped ZnO samples. This may be due to the increase in defect mediated recombination [23] taking place at the 10-20% aluminum doping level.

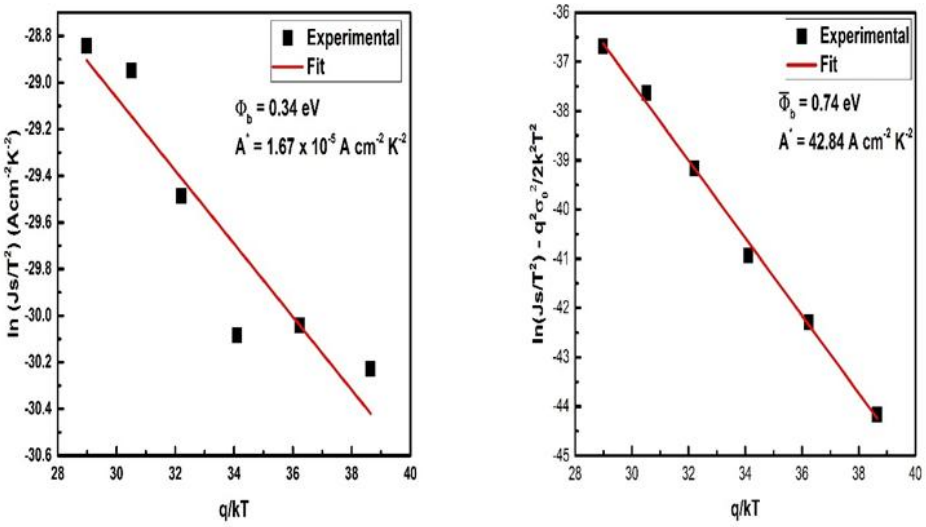

(a) **(b)**

Fig. 11 (a) Richardson plot **(b)** Modified Richardson plot for undoped ZnO

Table 1 Barrier height and ideality factor measured from I-V analysis from all samples.

Al Concentration (%)	Barrier height (eV)	Ideality Factor (n)
0	0.740	2.28
5	0.786	2.12
10	0.761	2.15
15	0.757	2.16
20	0.743	2.19

3.5Capacitance-Voltage (C-V) Measurement

Electrical properties of the heterojunctions were further investigated by capacitance-voltage (C-V) measurements in which C-V curves were plotted as a function of bias voltage at room temperature. We used the relation

$$(\frac{A}{C})^2 = \frac{-2(V_{bi}-V)}{q\varepsilon_0\varepsilon_r N_d} \qquad (9)$$

for estimating the built-in potential V_{bi}, and the dopant density N_d. InEqn. 9, we used the value of the dielectric constant $\varepsilon_r$forZnO as 9 and the density of the conduction band states asNc = 4.8 x 10^{18} cm^{-3} for ZnO [31]. The effective cell area, A of each sample was estimated as 8.2 x 4.6 mm^2. The dopant concentration N_d in various samples was estimated from the equation

$$N_d = \frac{-2}{q\varepsilon_0\varepsilon_r\,(slope\ of\ 1/C^2-V)} \qquad (10)$$

The barrier height φ_b in a heterojunction is related to the built-in voltage V_{bi} by a relation given by

$$\emptyset_b = V_{bi} + \frac{kT}{q} ln(\frac{N_C}{N_d}) \quad (11)$$

Table2 Barrier height and carrier concentration from C-V analysis

Al Concentration (%)	Barrier height (eV)	Carrier Concentration (cm^{-3})
0	0.852	9.25×10^{13}
5	0.886	5.83×10^{14}
10	0.872	6.38×10^{14}
15	0.863	8.37×10^{14}
20	0.863	8.45×10^{14}

Table 2 summarizes the barrier height and carrier concentration for all samples. As shown in Table 2, the barrier height increases from 0.852 eV to 0.886 eV for undoped to 5% doped samples. Aluminum incorporation in ZnO lattice reduces the number of oxygen vacancies and leads to lower density of free carrier, which in turn can effectively increase the barrier height at the junction interface [32]. The barrier height in Fig.13 shows an abrupt variation after 5% doping. These results are again consistently indicating anomalous values of junction parameters at 10-20% aluminum doping. The observed changes in junction parameters may be due to defects mediating the recombination process [23] taking place at higher aluminum doping. Fig. 12 (a) and (b) show the raw C-V data and the plot of $(A/C)^2$ vs V for various doped samples.

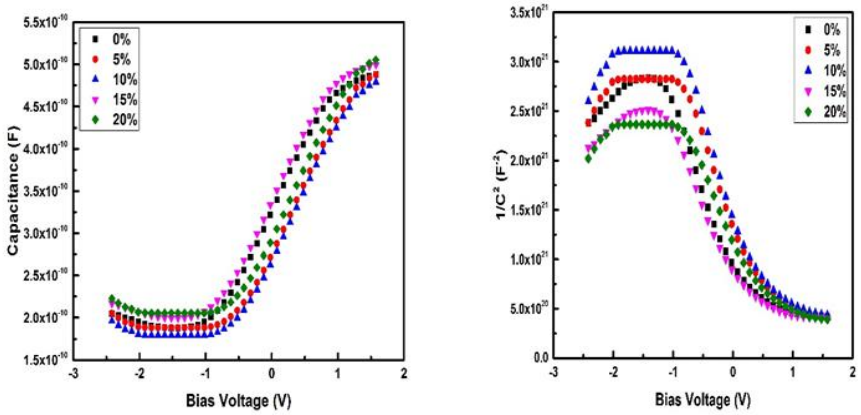

(a) (b)

Fig. 12 (a) C-V plot (b) $(A/C)^2$ – V plot

Fig. 13 compares the barrier height estimations based on I-V and the C-V measurements. These two electrical measurements yield barrier height values within 10-12 % and the changes with aluminum doping follows the same trend.

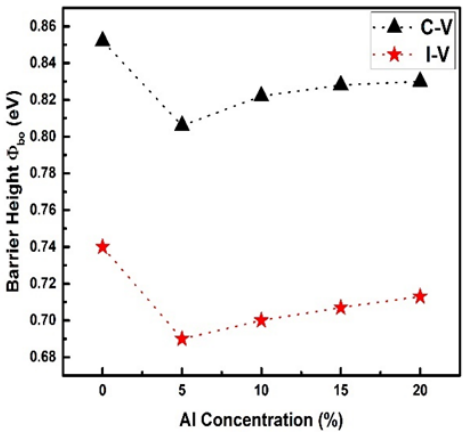

Fig. 13 Barrier height comparison from I-V and C-V measurements

VI. CONCLUSION

In conclusion, aluminum doped ZnO nanorods have been synthesized on a p-Si substrate using a chemical bath deposition technique. Average ZnO nanorods diameter decreases as the doping is increased from 0 to 20%.Aluminum doped ZnO/p-Si heterojunctions can be tuned to have band gap ranging from 3.31 eV (undoped) to 3.58 eV (20%). The optical properties from PL show blue shift in UV emission peak and decrease in both the impurity and oxygen related peaks as aluminum is introduced into the structure. One of the important results from electrical characterization is that beyond 5% doping, many of the junction characteristics degrade. Electrical measurements show that aluminum incorporation is improving the rectifying properties as the doping is increased up to 5%. The barrier height estimated from the I-V and C-V methods are quite similar and beyond 5% doping levels there is significant drop in the barrier height. Aluminum doping may be used to control the optical, structural, electrical, and transport properties of ZnO nanostructured/p-Si heterojunction.

ACKNOWLEDGEMENTS

The authors would like to thanks the funding agencies OK-NASA EPSCoR (project number NNX13AN01A and NNX15AM75A) and DOE ARPA-E for financial support. This work was also supported by the TU Nanotechnology and the Oklahoma Photovoltaic Research Institute

REFERENCES

[1] C. Periasamy, and P. Chakrabarti, Large-area and nanoscale n-ZnO/p-Si heterojunction photodetectors,*Journal of Vacuum Science & Technology B29*, 2011, 051206
[2] A. Janotti, and C. G. V. Walle, Fundamentals of zinc oxide as a semiconductor,*Rep. Prog. Phys. 72*, 2009, 126501.
[3] D. G. Georgiadou et al. Scalable fabrication of nanostructured p-Si/n-ZnO heterojunctions by femtosecond-laser processing." *Mater. Res. Express 1*, 2014, 045902.
[4] I. S. Jeong, J. H. Kim, and S. Im,Ultraviolet-enhanced photodiode employing n-ZnO/p-Si structure,*Appl. Phys. Lett.83*, 2003, 2946-2948.
[5] S. Mridha, and D. Basak, Ultraviolet and visible photoresponse properties of n- ZnO⁄p- Si heterojunction, *Journal of Applied Physics101*, 2007, 083102.
[6] J. D. Ye, S. L. Gu, S. M. Zhu, W. Liu, S. M. Liu,R. Zhang et.al., Electroluminescent and transport mechanisms of n-ZnO⁄p-Siheterojunctions,*Appl. Phys. Lett.88*, 2006, 182112.
[7] S. Al-Heniti, R. I.Badran, A. A. Al-Ghamedi, and F. A. Al-Agel,The Effect of Helium Dilution on Optical and Photoelectric Properties of a-Si: H Thin Films Prepared by Plasma Enhanced Chemical Vapor Deposition Technique,*Adv. Sci. Lett. 4*, 2011, 24.
[8] Z. Guo, D. X. Zhao, Y. C. Liu,D. Z. Shen,J. Y. Zhang, and B. H. Li, Fabrication and Electrical Characteristics of Individual ZnO Submicron-Wire Field-Effect Transistor, Appl. *Phys. Lett. 93*, 2008, 163501.
[9] L. Li, C. X. Shan, B. H. Li, B. Yao,D. Z. Shen,B. Chu, and Y. M. Lu, Light-Harvesting in n-ZnO/p-Silicon Heterojunctions, J. *Electron. Mater. 9*, 2010, 2467.
[10] J. H. He, S. T. Ho, T. B. Wu, L. J. Chen, and Z. L. Wang, Electrical and photoelectrical performances of nano-photodiode based on ZnO nanowires,*Chem. Phys. Lett. 435*, 2007, 119
[11] R. Ghosh, and D. Basak, Electrical and ultraviolet photo response properties of quasi aligned ZnO nanowires/p-Si heterojunction,*Appl. Phys. Lett. 90*, 2007, 243106.
[12] S. S. Shariffudin, M. H. Mamat, and M. M. Rusop, Growth of Self-Catalyzed ZnOHeterostructures using Thermal Chemical Vapor Deposition Method,*Advanced Materials Research667*, 2013,338-342.
[13] L. S. Zambom, and R. D. Mansano, p-ZnO Thin Films Deposited by RF-Magnetron Sputtering, *J. Phys.: Conf. Ser. 591*, 2015,012040.
[14] M. Quintana, E. Ricra, J. Rodríguez, W. Estrada, Spray pyrolysis deposited zinc oxide films for photo-electrocatalytic degradation of methyl orange: influence of the PH,*Catalysis Today*, *76*(2–4), 2002, 141-148.
[15] J. Rouhi, F. S.Husairi, K. A. Eswar, S. A. H. Alrokayan, H. A. Khan, and M. Rusop, Vertical Growth of ZnONanocone Arrays on Polycarbonate Substrate by Voltage-Assisted Chemical Bath Deposition,*Advanced Materials Research*, *1109*, 2015, 495-499
[16] H. M. Mohamad,I. C. K.Mohd, N. H. N. M. Nik et al., Effects of Annealing Environments on the Solution-Grown, Aligned Aluminium-Doped Zinc Oxide Nanorod-Array-Based Ultraviolet Photoconductive Sensor, *Journal of Nanomaterials,15*,2012, 189279
[17] O. Lupan, T. Pauporté, L. Chow, B. Viana, F. Pellé, L. K. Ono, B. R. Cuenya, and H. Heinrich, Effects of annealing on properties of ZnO thin films prepared by electrochemical deposition in chloride medium*Applied Surface Science*, *256*(6), 2010, 1895-1907.
[18] Y. Jr. Hung, S. L. Lee, K. C. Wu, Y. Tai, and Y. T. Pan, Antireflective silicon surface with vertical-aligned silicon nanowires realized by simple wet chemical etching processes,*Opt. Express 19*, 2011, 15792-15802.
[19] E. Burstein, Anomalous Optical Absorption Limit in InSb,*Phys. Rev.*, *93*(Feb), 1954, 632.
[20] T. S. Moss, Theory of the Spectral Distribution of Recombination Radiation from InSb, *Proc. Phys. Soc. B, 70*,1957, 247.
[21] O. Baka, A. Azizi, S. Velumaniet al., Effect of Al concentrations on the electrodeposition and properties of transparent Al-doped ZnO thin films, *J Mater Sci: Mater Electron*,*25*, 2014, 1761.
[22] R. Haarindraprasad, U. Hashim, S. C. B. Gopinath, M. Kashif, P. Veeradasan, S. R. Balakrishnan, andP. Poopalan, Low Temperature Annealed Zinc Oxide Nanostructured Thin Film-Based Transducers: Characterization for Sensing Applications,*PLoS ONE,10*(7),2015,0132755.
[23] J. J. Ding,H. X. Chen,andS. Y. Ma, Structural and photoluminescence properties of Al-doped ZnO films deposited on Si substrate,*PhysicaE: Low-dimensional Systems and Nanostructures*, 42(6), 2010, 1861-1864.
[24] X. Zhang,J. Qin,Y. Xue, P. Yu,B. Zhang,L. Wang,andL. Liu, Effect of aspect ratio and surface defects on the photocatalytic activity of ZnOnanorods,*Sci Rep.*, *4*(April), 2014, 4596
[25] N. Zebbar,Y. Kheireddine,K. Mokeddem, A. Hafdallah,M. Kechouane,andM. S. Aida,Structural, optical and electrical properties of n-ZnO/p-Si heterojunction prepared by ultrasonic spray,*Materials Science in Semiconductor Processing*, *14*(3–4),2011, 229-234

[26] D. Somvanshi, and S. Jit,Mean Barrier Height and Richardson Constant for Pd/ZnO Thin Film-Based Schottky Diodes Grown on n-Si Substrates by Thermal Evaporation Method, *IEEE Electron Device Letters*, *34*(10), 2013, 1238-1240
[27] S. Al-Heniti, R. I.Badran, A. A. Al-Ghamedi, and F. A. Al-Agel, The Effect of Helium Dilution on Optical and Photoelectric Properties of a-Si: H Thin Films Prepared by Plasma Enhanced Chemical Vapor Deposition Technique,*Adv. Sci. Lett*.,*4*, 2011, 24.
[28] A. Hussain, Temperature dependent current–voltage and photovoltaic properties of chemically prepared (p)Si/(n)Bi2S3 heterojunction,*Egyptian Journal of Basic and Applied Sciences3*(3), 2016, 314-321
[29] M. Nawaz, andA.Ahmad, Influence of absorber doping in a-SiC:H/a-Si:H/a-SiGe:H solar cells,*J. Semicond*.,*33*, 2012,042001
[30] U. Aeberhard, Quantum-kinetic Theory of Defect-mediated Recombination in Nanostructure-based Photovoltaic Devices, In *MRS Proceedings*, *1493*, 2013, 91–96.
[31] I. Hussain,M. Y. Soomro, N. Bano, O. Nur, and M. Willander, Interface trap characterization and electrical properties of Au-ZnOnanorodSchottky diodes by conductance and capacitance method,*Journal of Applied Physics*,*112*, 2012, 064506
[32] İ. Taşçıoğlu,W. A. Farooq,R. Turan, S. Altındal,andF. Yakuphanoglu,Charge transport mechanisms and density of interface traps in MnZnO/p-Si diodes,*Journal of Alloys and Compounds*,*590*(25), 2014, 157-161.